Application of Notch Filter Design for Being Compensators in Mechanical Gimbal Systems

Ing-Jiunn Su[1], Yau-Hwa Tseng[1*] and Karl Yung-Ta Huang[2]

[1] *Department of Electrical and Electronic Engineering, Chung Cheng Institute of Technology National Defense University, Taoyuan, Taiwan*
[2]*Electronic Systems Research Division, Chung-Shan Institute of Science and Technology, Taoyuan, Taiwan*

ABSTRACT

In the control system, notch filters can reduce the mechanical resonances of the plant at frequencies above the normal (or the margin) upper unity gain frequency. Let the gradual higher frequency sinusoidal signal be the command which inputs in the position and rate loop, an experiment of frequency response for the mechanical gimbal system in arbitrary elevation and azimuth angles can be practiced. Based on the result of the magnitude/phase response, some notch filters are utilized to eliminate the spike at specific frequencies whose design methods of transfer function and analogue circuit realization are summarized. Furthermore, a prototype implementation method of servo control system is given. Following the experimental structure, an example and the comparison of the frequency response before/after compensating will be presented in this paper.

Keywords: notch filter, servo control system, Butterworth filter, Chebyshev filter, inverse Chebyshev filter, frequency transformation, general impedance convertor (GIC) circuit.

陷波濾波器設計應用於機械式環架系統之補償器

蘇英俊[1]　曾耀華[1*]　黃勇達[2]

[1]國防大學理工學院電機電子工程系
[2]中山科學研究院電子系統研究所

摘　要

於控制系統中，陷波濾波器可消除待測物的機械共振頻率高於正歸化值或者是邊界值之頻率信號，利用漸高頻率之弦波信號為命令，輸入至位置迴路與速度迴路中，其待測機械環架系統於任意水平與垂直角度頻率響應即可實驗之。基於前述實驗所得之大小與相位響應結果，陷波濾波器即被用來濾除特定頻率之突波，而其轉移函數及類比電路的實現設計方法將統整於本論文中。除此之外，本文亦提供一種典型的伺服控制系統電路方法來實現之。根據前述之實驗架構，將於本文舉例並比較補償前後頻率響應之實測資料。

關鍵詞：陷波濾波器，伺服控制系統，巴特沃斯濾波器，柴比雪夫濾波器，反式柴比雪夫濾波器，頻率轉換，一般性阻抗轉換器電路

文稿收件日期 103.06.10;文稿修正後接受日期 104.04.22; *通訊作者
Manuscript received June 10, 2014; revised April 22, 2015; * Corresponding author

I. INTRODUCTION

For frequency domain analysis, if the received radio signal in the desired band is passed through and simultaneously attenuating the rest of signal, the filter design must be invented and applied. For example, in data conversion, filters are employed for restraining the effects of aliases in analog-to-digital (A/D) systems. They are used for reconstruction of the signal at the output in digital-to-analog (D/A) systems as well. In addition, for smoothing the waveform in the spectrum, the sampling frequency component and its harmonics must be eliminated in the image processing ([1]-[3]). Notch filters are also designed for removing the periodic noises in the image ([4]) and reducing blocking artifact from discrete cosine transform (DCT) coded image ([5]).

The function of gimbal systems is shown in Fig. 1. When the antenna receives the echo, the servo module will carry out the mandate form the digital signal processing (DSP) module. Then the gimbal system will be driven until the angle/rate approaches to the command. Attending to the coordinate of the aim is defined by the elevation and azimuth axis. For maintaining the steadiness of the system, the notch filter has been designed and applied to the missile system ([6]-[12]).

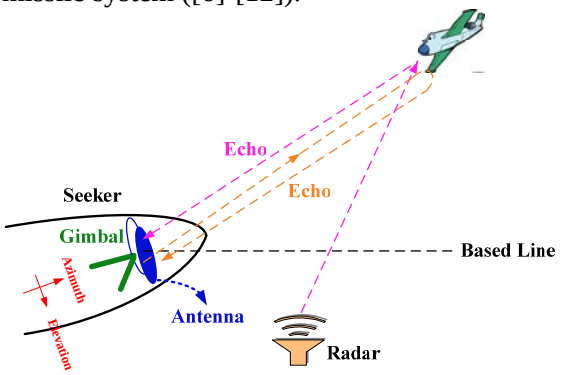

Fig.1. The function of gimbal systems in the seeker.

In the assembly gimbal system involving in servo controllers, the one of reasons of hunting effect is caused by the revolving frequency of the sensor and the corresponding harmonic wave frequency. Velocity and position transducers are presented as information feedback elements for closed loop control. Thus, it will interfere with the stability and degrade the performance of the system. The natural frequency of the mechanism must be rejected as well, where the location of the natural frequency depends on the mass distribution and quality of fabrication. The above-mentioned frequencies bring on the surplus peak in the spectrum and then the distorted signal is received. Furthermore, other periodic signals will be associated with the gimbal behavior.

In this paper, the second and higher order notch filter approach will be illustrated by many methods. It includes the transfer function derivation of the notch filter and implements to the firmware. However, if the plenty delay is employed in the control loop such that the microprocessor control unit (MCU) can't finish calculating in the sampling duration or the format of sensor output is differential voltage, the passive or active analog circuit of notch filters could be auxiliary to be the compensator in the gimbal system.

The organization of this paper is as follows. In section II, the standard second-order transfer function and the passive circuit realization of notch filter are modeled. A design example is following given. In section III, prototype filters are introduced first. Based on these models, the corresponding transfer function of multiple order notch filters can be evaluated by the frequency transformation method. In section IV, some active circuits with OP amplifier which are developed by RC resonant circuit are presented. Then, the hardware improvement and a design example are presented in section V. Finally, conclusions are drawn in section VI.

II. SECOND-ORDER NOTCH FILTERS AND THEIR CHARACTERISTICS

The second-order filtering function with notch frequency, f_a, and 3-dB bandwidth, *BW*, is given by ([13], [14])

$$H_{NF}(s)=\frac{s^2+s\times 2\pi f_a/Q'+(2\pi f_a)^2}{s^2+s\times 2\pi f_a/Q+(2\pi f_a)^2},Q'>Q$$
$$=\frac{s^2+s\times 2\pi f_a/Q'+(2\pi f_a)^2}{s^2+s\times 2\pi\cdot BW+(2\pi f_a)^2}, \quad (1)$$

where the pole Q $(Q=f_a/BW)$ factor represents the distance between the poles and

imaginary axis such that the poles are at $(-\pi \cdot BW) \pm j(2\pi f_a)$. Q' is the damping of the second-order transfer function which determines the bandwidth and depth of the notch filter. Let $Q' = \infty$, the 3-dB bandwidth of the regular notch filter is [15]

$$BW = 2\pi f_a \sqrt{1+\frac{1}{Q^2}+\frac{1}{Q}\sqrt{1+\left(\frac{1}{2Q}\right)^2}} - 2\pi f_a \sqrt{1+\frac{1}{Q^2}-\frac{1}{Q}\sqrt{1+\left(\frac{1}{2Q}\right)^2}} \quad (2)$$

Following (1), the value of the high and low frequency gain can be found to be unity. Fig. 2 gives the ideal RLC circuit used for notch filter with the infinite impedance at $2\pi f_a = 1/\sqrt{LC}$, that causes zero transmission at this frequency.

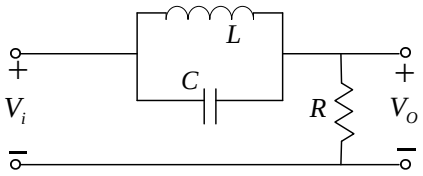

Fig.2. The circuit realization of the regular notch filter.

The shunt impedance is resistive and thus doesn't introduce transmission zeros. It follows that the circuit shown in Fig. 2 will realize the transfer function. ([13], [16], [17])

$$H_{NF}(s) = \frac{s^2 + (1/(LC))^2}{s^2 + s/(RC) + (1/(LC))^2}. \quad (3)$$

It's observed that when s approaches to zero and infinity, the limitation of (3) is unity. Another circuit implementation of notch filter without inductance is given by Fig. 3. The transfer function is ([16])

$$H_{NF}(s) = \frac{s^2 + \frac{s}{R_{16}C_8} + \frac{s}{R_{14,15}C_8} + \frac{1}{R_{15}R_{16}C_7C_8}}{s^2 + \frac{s}{R_{16}C_8} + \frac{s}{R_{14,15}C_8} + \frac{s}{R_{13,16}C_7} + \frac{R_{13}+R_{14,15}+R_{16}}{R_{13}R_{14,15}R_{13,16}C_7C_8}} \quad (4)$$

where $R_{13,16} = R_{13} // R_{16}$ and $R_{14,15} = R_{14} // R_{15}$. Here the parameters of s at numerator and denominator represent adjustable damping values that can regulate the depth and bandwidth of notch filter. Passive models of notch filters can be applied to filter the synchronized frequency of switching power transformation.

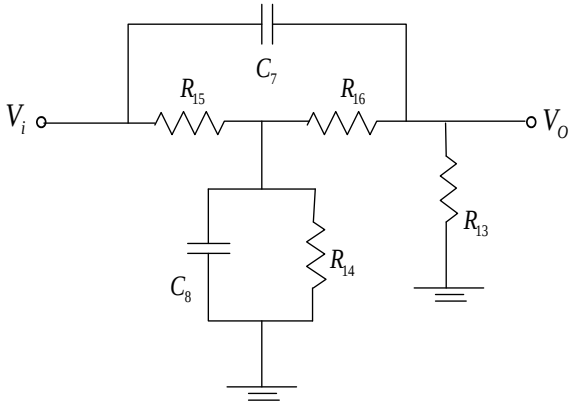

Fig.3. The passive notch filter circuit realization without inductance.

Consider the design example for f_a = 267Hz and 534Hz (the harmonic frequency of the rate sensor), then the 3dB bandwidth (78.6225Hz, 311.6254Hz) of notch filters is given. The corresponding transfer function can be evaluated by (1). Based on bode diagrams in Fig. 5 and Fig. 6, the depth of two notch filters are $20\log(0.0016) = -55.918$ dB and $20\log(0.0002257) = -72.919$ dB, respectively. The specification of two analog notch filters is summarized in Table. 1.

Table 1. Specification of second-order regular notch filter ($Q' = \infty$)

f_a	267 Hz	534 Hz
BW	78.6225 Hz	311.6254 Hz
Zeros	$\pm 1677.6i$	$\pm 3355.2i$
Poles	$-247 \pm 1659.3i$	$-979 \pm 3209.2i$
Depth	55.918 dB	72.929 dB
Peak time	37.5 ms	37.3 ms
Overshoot %	14%	13.5%
Settling time	45.5 ms	39.5 ms
Rise time	31 ms	32 ms
Phase lag	-2.6 degree	-2.536 degree

The effect of the damping ratio is compared in Fig. 4 and Fig. 5. It's observed that the higher the damping ratio, the shallower the depth, but the smaller the phase delay.

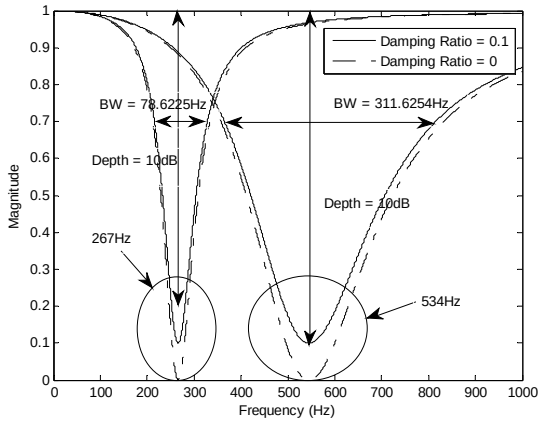

Fig.4. Comparison of the magnitude response of different transfer functions.

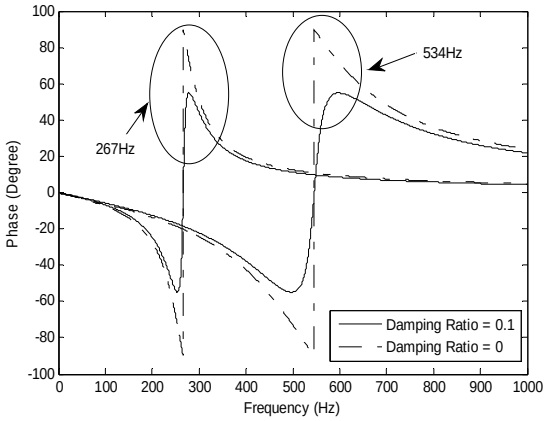

Fig.5. Comparison of the phase response of different transfer functions.

III. HIGHER ORDER NOTCH FILTERS AND THEIR CHARACTERISTICS

The transfer function of multi-order notch filter can be obtained from the cascaded double notch filter. However, to design more suitable (or odd order) notch filter functions, classical transfer functions of low pass filter (LPF) must be the reference models, then notch filter functions can be evaluated by the frequency transformation of the classical prototype transfer function.

3.1 Butterworth Low Pass Filter

The Butterworth filter without ripple in the pass and stop band is the best compromise attenuation and phase response. However, the Butterworth filter achieves its flatness at the expense of a relatively wide transition region from pass and stop band. For continuous-time Butterworth filters, the poles associated with square of the magnitude of the frequency response are equally distributed in angle on a circle in the S-plane, concentric with the origin and having a radius equal to the cutoff frequency (approximately the 3 dB frequency). When the cutoff frequency and the filter order have been specified, the poles characterizing the system function are readily obtained. Once the poles are specified, it is straightforward to obtain the differential equation characterizing the filter.

The normalized *N*-th order Butterworth polynomial, $B_N(s)$, has the following general form ([13], [17])

$$B_N(s)=\begin{cases}\displaystyle\prod_{k=1}^{N/2}\left[s^2-2s\cos\left(\frac{2k+N-1}{2N}\pi\right)+1\right], \\ \text{for } N \text{ even} \\ \displaystyle(s+1)\prod_{k=1}^{\frac{(N-1)}{2}}\left[s^2-2s\cos\left(\frac{2k+N-1}{2N}\pi\right)+1\right], \\ \text{for } N \text{ odd}\end{cases} \tag{5}$$

,where $s=j\omega/\omega_c$ with cutoff frequency ω_c. Therefore, the normalized Butterworth polynomial can be employed to determine the transfer function with direct current (DC) gain $G_{0,But}$ for any low pass filter as follows.

$$H_{But}(s)=G_{0,But}/B_N(s/\omega_c) \tag{6}$$

Separating (5), the factor of polynomial is listed in Table 2.

Table 2. Factor of Butterworth polynomial

Order	Factor of Polynomial
1	$s+1$
2	$s^2+1.414s+1$
3	s^3+2s^2+2s+1
4	$s^4+2.61s^3+3.41s^2+2.61s+1$
5	$s^5+3.24s^4+5.24s^3+5.24s^2+3.24s+1$

Let $A_{p,dB}$ be the maximum variation in pass-band transmission, then the magnitude for an *N*-th order Butterworth filter with a passband edge, w_c is given by ([13], [17])

$$\left|H_{But}(s)\right| = \left[1 + (10^{A_{p,dB}/10} - 1)(\omega/\omega_c)^{2N}\right]^{-1/2} \quad (7)$$

3.2 Chebyshev Low Pass Filter

The Chebyshev filter (Chebyshev Type I filter) has a smaller region than the same order Butterworth filter at the expense of ripples in its pass band. This filter minimizes the height of maximum ripple, which is the Chebyshev criterion. Let $R_{p,dB}$ be the pass band ripple in dB, the *i*-th complex pole value for the *N*-th order Chebyshev filter transfer function can be written as $P_{Che,i} = K_{R,i} + jK_{I,i}$ ($i = 1,...,N$), where

$$K_{R,i} = -\sinh\left(\frac{\sinh^{-1}(10^{R_{p,dB}/10} - 1)^{-1/2}}{N}\right)\sin\left(\frac{2i-1}{2N}\pi\right) \quad (8)$$

and

$$K_{I,i} = \cosh\left(\frac{\sinh^{-1}(10^{R_{p,dB}/10} - 1)^{-1/2}}{N}\right)\cos\left(\frac{2i-1}{2N}\pi\right) \quad (9)$$

,respectively [17]. Then the non-zero transfer function of Chebyshev LPF can be characterized by

$$H_{Che}(s) = G_{0,Che} \Big/ \prod_{i=1}^{N}\left(s - P_{Che,i}\right) \quad (10)$$

where the calibrated gain

$$G_{0,Che} = \begin{cases} 10^{-R_{p,dB}/20}\prod_{i=1}^{N}\left(-P_{Che,i}\right), & \text{for } N \text{ even} \\ \prod_{i=1}^{N}\left(-P_{Che,i}\right), & \text{for } N \text{ odd} \end{cases} \quad (11)$$

such that the DC gain (i.e. the width of the ripple) is $10^{-R_{p,dB}/20}$ and the 3dB bandwidth is $\cosh((1/N)\cosh^{-1}(1/\sqrt{10^{R_{p,dB}/20} - 1}))$. Therefore, $R_{p,dB} = 3.01$ must be assigned to keep the bandwidth on the desired frequency.

The magnitude response of an *N*-th order Chebyshev filter with a passband edge (ripple bandwidth) w_c is given by ([13], [17])

$$\left|H_{Che}(s)\right| = \begin{cases} \dfrac{10^{-R_{p,dB}/20}}{\cos[N\cos^{-1}(\omega/\omega_c)]}, \text{when } \omega \le \omega_c \\ \dfrac{10^{-R_{p,dB}/20}}{\cosh[N\cos^{-1}(\omega/\omega_c)]}, \text{when } \omega \ge \omega_c \end{cases} \quad (12)$$

3.3 Inverse Chebyshev Low Pass Filter

Inverse Chebyshev analog filter is also known as Chebyshev analog filter of the second kind. The frequency response of this filter monotonously falls in the passband and transition region. Similar to Butterworth filter, the frequency response is extremely flat function at 0 Hz. In the stop band, inverse Chebyshev filter has the least oscillation in the frequency response.

Let $\varepsilon = 1/\sqrt{10^{R_{s,dB}/10} - 1}$ with $R_{s,dB}$ decibels of ripple in the stop band, the *i*-th pole of *N*-th order inverse Chebyshev polynomial is located at [17]

$$\begin{aligned} P_{IChe,i} &= 1/P_{Che,i}, i = 1,\cdots,N \\ &= \frac{-\sinh(U)\sin(V) - j\cosh(U)\cos(V)}{\sinh^2(U)\sin^2(V) + \cosh^2(U)\cos^2(V)}, \end{aligned} \quad (13)$$

where

$$U = (1/N)\sinh^{-1}(1/\varepsilon);$$
$$W = (2i-1)\pi/(2N).$$

The *k*-th zero is given by

$$Z_{IChe,k} = \sec W, \begin{cases} k = 1,\cdots,\dfrac{N-1}{2}, \text{for } N \text{ odd} \\ k = 1,\cdots,\dfrac{N}{2}, \text{for } N \text{ even} \end{cases} \quad (14)$$

The value of zeros determines the location of the notch frequency. Then, the transfer function of Chebyshev type II LPF model can be expressed as

$$H_{IChe}(s) = \begin{cases} \dfrac{\prod_{i=1}^{N}\left(-P_{IChe,i}\right)\prod_{k=1}^{(N-1)/2}\left(s^2 + Z_{IChe,k}^2\right)}{\prod_{k=1}^{(N-1)/2} Z_{IChe,k}\prod_{i=1}^{N}\left(s - P_{IChe,i}\right)}, \text{for } N \text{ odd} \\ \dfrac{\prod_{i=1}^{N}\left(-P_{IChe,i}\right)\prod_{k=1}^{N/2}\left(s^2 + Z_{IChe,k}^2\right)}{\prod_{k=1}^{N/2}\left(s - P_{IChe,k}\right)\prod_{i=1}^{N}\left(s - P_{IChe,i}\right)}, \text{for } N \text{ even} \end{cases} \quad (15)$$

The magnitude response of *N*-th order inverse Chebyshev filter with cutoff frequency ω_c is obtained by replacing ω/ω_c by ω_c/ω in (15), that is ([18], [19])

$$|H_{ICh e}(s)| = \begin{cases} \dfrac{\varepsilon^2 \cosh^2\left[N\cos^{-1}(\omega_c/\omega)\right]}{1+\varepsilon^2\cosh^2\left[N\cos^{-1}(\omega_c/\omega)\right]} \\ ,\text{when } \omega \le \omega_c \\ \dfrac{\varepsilon^2 \cos^2\left[N\cos^{-1}(\omega_c/\omega)\right]}{1+\varepsilon^2\cos^2\left[N\cos^{-1}(\omega_c/\omega)\right]} \\ ,\text{when } \omega \ge \omega_c \end{cases} \quad (16)$$

For a design example of fourth order low pass filter at 267 Hz, let the ripple level of pass-band/stop-band for Chebyshev/inverse Chebyshev be 3dB. Thus $R_{p,dB} = 3$ and $R_{s,dB} =$ 10.458 are determined, respectively. The corresponding results of Bode diagrams are shown in Fig. 6 and Fig. 7. Particularly for the inverse Chebyshev filter, the ripple has double notch filter characteristic when the deep ripple level is given. The compensator can save more firmware computation if the ripple locates at the desired frequency.

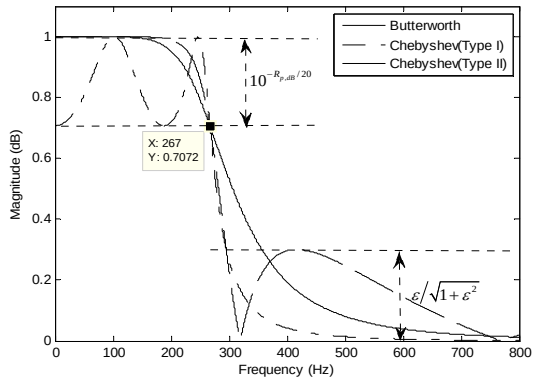

Fig.6. Magnitude response of 267 Hz fourth order analog prototype LPF.
($R_{p,dB} = 3$, $R_{s,dB} = 10.458$)

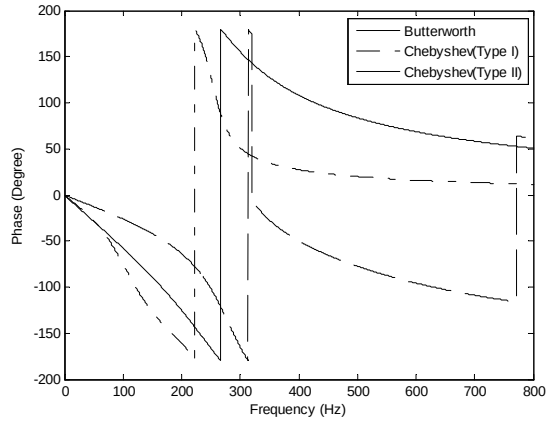

Fig.7. Phase response of 267 Hz fourth order analog prototype LPF. ($R_{p,dB} = 3$, $R_{s,dB} = 10.458$)

Finally, by translating all of *s* in the transfer function shown in (6), (10), and (15) into $s \cdot BW/(s^2 + (2\pi f_a)^2)$, the multi-order notch filter transfer function can be obtained.

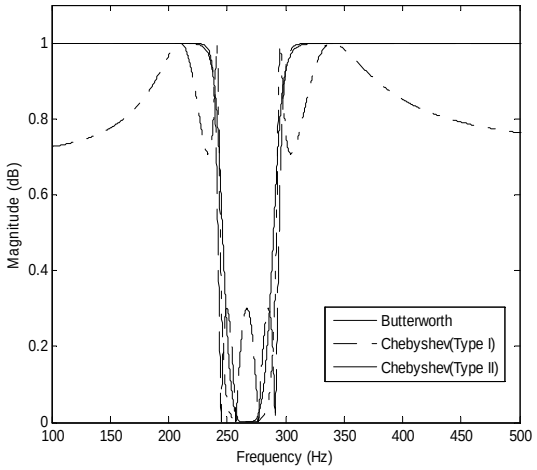

Fig.8. Magnitude response of the 267 Hz eighth order notch filter.

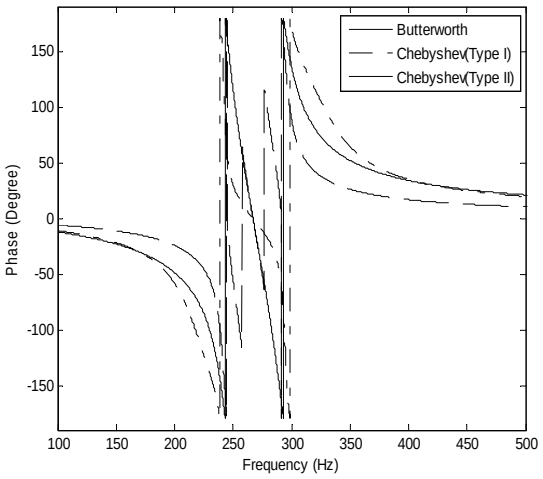

Fig.9. Phase response of the 267 Hz eighth order notch filter.

Following the previous design example, 267 Hz notch filters can be evaluated by using the LPF transformation method whose Bode diagrams are given in Fig. 8 and Fig. 9. Notice that, the ripple in the stop band is generated by the inverse Chebyshev LPF model. On the contrary, the stop band is flat for the Chebyshev filter. Furthermore, the inverse Chebyshev filter has the lowest phase lag among the filters. Finally, the specification is listed in Table 3.

Table 3. Specification of the 267Hz notch filter with BW = 78.6Hz

Filter Type	Butterworth	Chebyshev I	Chebyshev II
Zeros	$\pm 1677.6i$	$\pm 1677.6i$	$\pm 1677.6i$ $228.96 \pm 1662.017i$ $94.52 \pm 1674.95i$
Poles	$-81.7 \pm 1462.3i$ $-107.2 \pm 1918.7i$ $-215.2 \pm 1570.2i$ $-241.2 \pm 1759.3i$	$-19.7 \pm 1438.4i$ $-26.8 \pm 1956.2i$ $-184.9 \pm 1236.7i$ $-332.9 \pm 2225.9i$	$-39.05 \pm 1442.37i$ $-52.78 \pm 1949.78i$ $-103.9 \pm 1572.17i$ $-117.8 \pm 1782.33i$
Peak time	0.1826 s	0.1742 s	0.1845 s
Overshoot %	24.7%	33.5%	32.7%
Settling time	0.205 s	0.2169 s	0.2166 s
Rise time	0.16 s	0.1517 s	0.1593 s
Gain (40Hz)	0 dB	-2.98 dB	0 dB
Phase lag (40Hz)	-4.297 degree	-3.767 degree	-2.088 degree

(*Chebyshev I：Chebyshev Type I Filter；Chebyshev II：Inverse Chebyshev Filter)

IV. ACTIVE CIRCUIT REALIZATIONS OF SECOND ORDER NOTCH FILTERS

Consider the analogue notch filter illustrated in Fig. 10, the input voltage V_i is given and assume the working circuit is producing a finite output voltage, V_o.

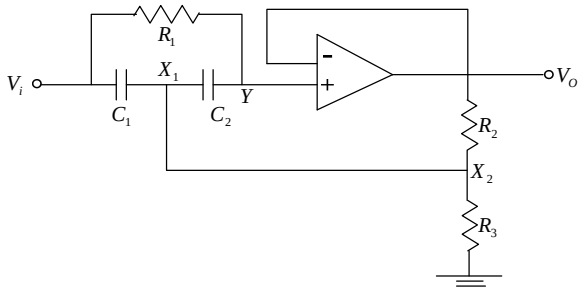

Fig.10. Analogue second-order notch filter (Example I).

For calculating the closed-loop transfer function, let V_{X_1}, V_{X_2} and V_Y be the voltage in X_1, X_2 and Y. Then, the current through X_2 is determined as

$$\frac{V_Y - V_{X_2}}{R_2} + \frac{V_Y - V_{X_1}}{1/(sC_2)} + \frac{V_i - V_{X_1}}{1/(sC_1)} = \frac{V_{X_2}}{R_3} \qquad (17)$$

Due to the virtual short property, $V_Y = V_0$, the node equation at Y is given by

$$V_{X_1} = \left((1 + R_1 sC_2)V_O - V_i\right) / \left(R_1 sC_2\right) \qquad (18)$$

By substituting (18) into (17), the analogue transfer function, $H_{NF}(s)$, is evaluated as

$$H_{NF}(s) = V_O / V_i$$
$$= \frac{C_1 C_2 R_1 R_{eq} s^2 + R_{eq}(C_1 + C_2)s + 1}{C_1 C_2 R_1 R_{eq} s^2 + R_{eq}(C_1 + C_2)s + s R_1 R_{eq} C_2 / R_3 + 1} \qquad (19)$$

where R_{eq} means the parallel resistant of R_2 and R_3. The detailed derivation of (19) is given by Appendix A. For simplifying and describing the physical meaning of the above equation, we define $Q(\omega_a, G) = (s/\omega_a)^2 + 2G(s/\omega_a) + 1$, where ω_a is the analog notch frequency (rad/s) and G can be utilized to estimate the depth of notch filter. The voltage gain can be written in the form

$$H_{NF}(s) = \frac{Q\left(1/\sqrt{R_1 R_{eq} C^2}, \sqrt{R_{eq}/R_1}\right)}{Q\left(1/\sqrt{R_1 R_{eq} C^2}, (1 + R_1/(2R_3))\sqrt{R_{eq}/R_1}\right)} \qquad (20)$$

where $C_1 = C_2 = C$ is considered. The corresponding depth of the notch filter is

$$D = \frac{1}{1 + R_1/(2R_3)} = \frac{2R_3}{R_1 + 2R_3} \tag{21}$$

It means that the depth of the notch filter depends on the value of R_1 and R_3. With $R_1 = 100K\Omega,\quad R_2 = 90.9K\Omega,\quad R_3 = 5.62K\Omega,$ $C_1 = C_2 = 0.1\mu F$, the ratio of V_O and V_i can be reduced to

$$H_{NF}(s) = \frac{s^2 + 200.6035s + 1.117568\times10^7}{s^2 + 2006.349s + 1.117568\times10^7} = \frac{Q(2\pi\times534, 0.03)}{Q(2\pi\times534, 0.3)} \tag{22}$$

The representation shows that the notch frequency occurs at 534Hz (the harmonic of rate sensor) and the depth is $20\log(0.03/0.3) = -20dB$. The corresponding bandwidth is 311.6254Hz.

The other example of analogue notch filter by using parallel capacitors is depicted in Fig. 11.

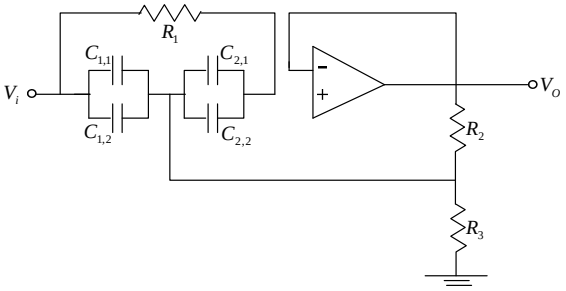

Fig.11. Analogue second-order notch filter (Example II).

Similar to (19) and (20), the transfer function is given by

$$H_{NF}(s) = V_O/V_i = \frac{C_1'C_2'R_1R_{eq}s^2 + C_1'R_{eq}s + C_2'R_{eq}s + 1}{C_1'C_2'R_1R_{eq}s^2 + R_{eq}(C_1' + C_2')s + R_1R_{eq}C_2's/R_3 + 1}, \tag{23}$$

where $C_1' = C_{1,1} + C_{1,2}$, $C_2' = C_{2,1} + C_{2,2}$. For the symmetrical case of C_1' and C_2', i.e. $C_1' = C_2' = C'$, (23) can be reduced to

$$H_{NF}(s) = \frac{Q\left(1/\sqrt{R_1R_{eq}C'^2}, \sqrt{R_{eq}/R_1}\right)}{Q\left(1/\sqrt{R_1R_{eq}C'^2}, (1 + R_1/(2R_3))\sqrt{R_{eq}/R_1}\right)}, \tag{24}$$

In this example, the voltage gain can be written as

$$\frac{V_O}{V_i} = \frac{s^2 + 100.3195s + 2.795584\times10^6}{s^2 + 501.6s + 2.795584\times10^6} = \frac{Q(2\pi\times267, 0.03)}{Q(2\pi\times267, 0.15)} \tag{25}$$

where the case of $R_1 = 100K\Omega,\quad R_2 = 90.9K\Omega,$ $R_3 = 12.1K\Omega,$ and $C_{1,1} = C_{1,2} = C_{2,1} = C_{2,2} = 0.1$ μF are employed. The representation also shows that the notch frequency occurs at 267Hz and the depth is $20\log(0.03/0.15) = -14$dB. Notice that the 3-dB bandwidth is 78.6225Hz. The specification of notch filter circuits with 267 Hz and 534 Hz is illustrated in Table. 4.

Table 4. Specification of second-order regular notch filter ($Q' \neq \infty$)

f_a	267 Hz	534 Hz
BW	78.6225 Hz	311.6254 Hz
Zeros	$-50 \pm 1671.2i$	$-100.3 \pm 3341.5i$
Poles	$-247 \pm 1659.3i$	$-979 \pm 3209.2i$
Depth	-14 dB	-20 dB
Peak time	37 ms	37.5 ms
Overshoot %	5.1%	13.1%
Settling time	41 ms	39.3 ms
Rise time	32 ms	29 ms
Phase lag	-2.113 degree	-2.338 degree

The other type notch filter circuit is given by Fig. 12.

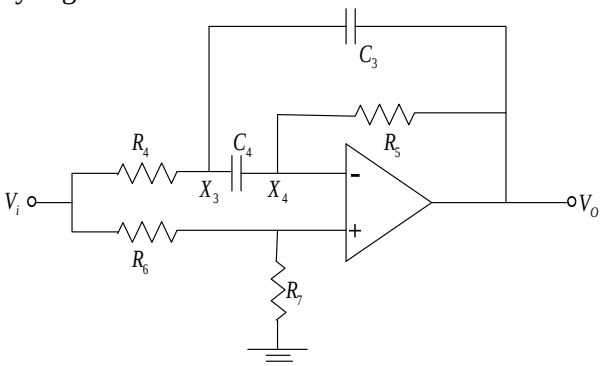

Fig.12 Analogue second-order notch filter (Example III)

The current through X_3 is determined by

$$\frac{V_i - V_{X_3}}{R_4} = \frac{V_{X_3} - V_O}{1/(sC_3)} + \frac{V_{X_3} - V_{X_4}}{1/(sC_4)} \quad (26)$$

where V_{X_3} and V_{X_4} are the voltage of node X_3 and X_4. A node equation at X_4 yields the current

$$(V_{X_3} - V_{X_4})/(1/(sC_4)) = (V_{X_4} - V_O)/R_5 \quad (27)$$

Assume that the OP amplifier is ideal with infinite gain, a virtual short circuit exists between its two input terminals. Hence the voltage at X_4 is characterized by

$$V_{X_4} = R_7 V_i/(R_6 + R_7) \quad (28)$$

Thus, by substituting (28) into (26) and (27), the transfer function for the circuit in Fig. 12 is evaluated by

$$H_{NF}(s) = V_O/V_i = [R_7/(R_6 + R_7)] \times \frac{C_3C_4R_4R_5s^2 + (R_4C_3 + C_4R_4 - C_4R_5R_6/R_7)s + 1}{C_3C_4R_4R_5s^2 + (C_3 + C_4)R_4s + 1} \quad (29)$$

The proof of (29) is given by Appendix B. Let $C_3 = C_4 = C$, (29) can be reduced to

$$\frac{V_O}{V_i} = \frac{R_7}{R_6 + R_7} \frac{Q\left(\frac{1}{\sqrt{R_4R_5C^2}}, \frac{(R_4 + R_5R_6/(2R_7))}{\sqrt{R_4R_5}}\right)}{Q\left(1/\sqrt{R_4R_5C^2}, \sqrt{R_4/R_5}\right)} \quad (30)$$

where $1/\sqrt{R_4R_5C^2}$ indicates the notch frequency and the corresponding depth of the notch filter is

$$D = R_7/(R_6 + R_7) + R_5R_6/(2R_4(R_6 + R_7)) \quad (31)$$

According to the result in (29), the depth of the notch filter depends on the value of resistances without capacitors. In the other hand, the deepest case of the notch filter is

$$R_4C_3 + C_4R_4 - C_4R_5R_6/R_7 = 0 \quad (32)$$

It also means that the depth of this filter is infinity when (32) is given.

In addition, the generalized impedance convertor (GIC) using double OP amplifiers circuit shown in Fig. 14 is sometimes used to implement the ideal notch filter. This circuit provides high quality inductance simulation whose transfer function is given by ([11], [15])

$$H_{NF}(s) = K_H \frac{s^2 + \frac{R_{11}}{C_5C_6R_9R_{10}R_{12}}}{s^2 + \frac{1}{C_5R_8}s + \frac{R_{11}}{C_5C_6R_9R_{10}R_{12}}}. \quad (33)$$

It's observed that X_5 shown in Fig. 13 is not a convenient node to use as the filter output terminal since connecting a load would change the characteristics of the filter. It can be solved by utilizing a buffer amplifier. Moreover, the value of buffer amplifier K_H can also be selected appropriately for the desired gain in the high and low frequency region.

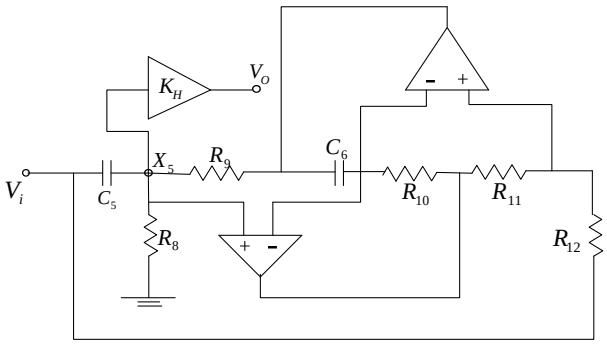

Fig.13. Analogue second-order notch filter (Example IV).

V. REALIZATION STRUCTURE AND MEASURED DATA OF GIMBAL SYSTEMS

Fig. 14 shows the control flow block and motor characteristics of a gimbal system. After receiving the data from sensors and the mode command, the compensation train is executed in MCU chip. Then the result is send to pulse width modulation (PWM) IC and power amplifier which is employed to drive the DC motor, where the DC motor with relative high inertia is used for driving the gimbal. The energy stored in the inertia is used during the transient period of load acceleration and deceleration. Thus, the motor weight is reduced and its rating parameters are determined more by the steady state conditions of loading.

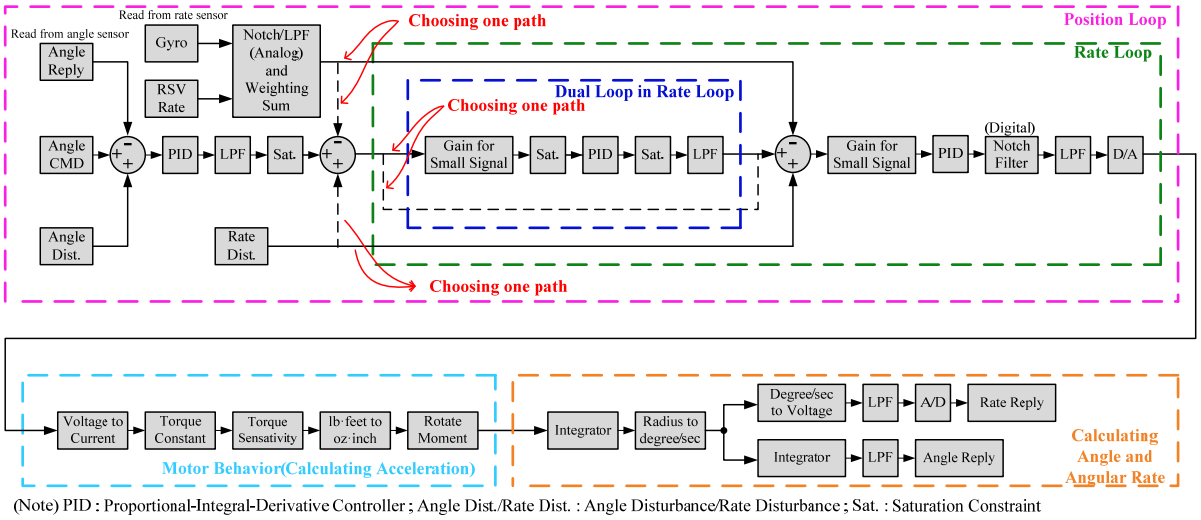

Fig.14. Simulation model of the mechanical gimbal system.

To verify the performance of a proposed scheme, a prototype implementation of the brush DC motor as shown in Fig. 15. The power amplifier stage includes a PWM IC with delay circuit, power driver circuit and current detected circuit. The control stage is based on a MCU microprocessor which is a 16-bits fixed point 10-MHz chip. It can perform all necessary controls such as the position and rate loop calculation. The field-programmable gate array (FPGA) is used to receive the command from DSP module and transmit all digital data. In addition, it supplies the necessary signal to resolver, resolver-to-digital (R2D) IC being the excitation signal, A/D and D/A IC.

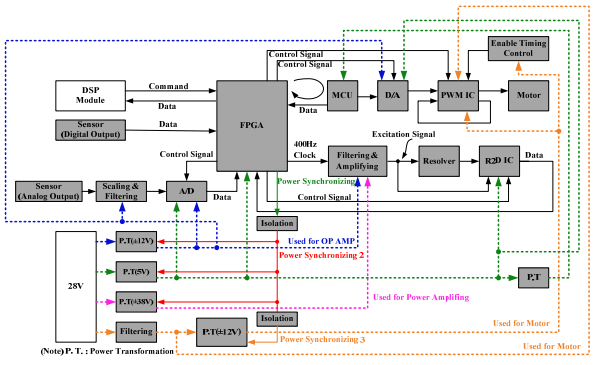

Fig.15. The hardware structure for implementing in mechanical gimbal system.

Let the gradual higher frequency sinusoidal signal be the disturbance which inputs in the rate loop, the measured magnitude and phase response versus frequency of the mechanical gimbal system is shown in Fig. 16 and Fig. 17. Notice that the gain margin is 6.2 dB and phase margin locates at 48.2 degrees at 40 Hz, respectively.

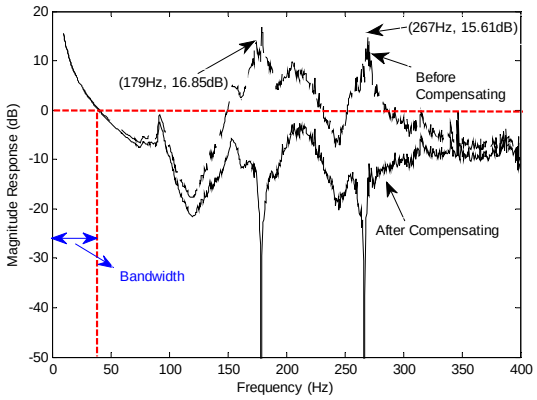

Fig.16. The comparison of magnitude response between with/without compensating.

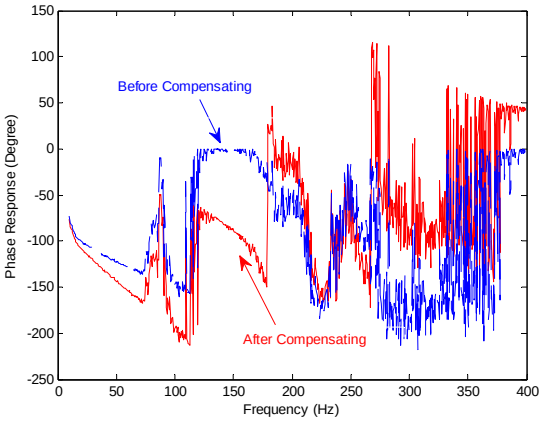

Fig.17. The comparison of phase response between with/without compensating.

For satisfying the specification of the servo system, such as the gain margin, phase margin

and bandwidth of the loop controller, notch filters must be chosen for being the compensator prior than LPF whose cutoff frequency locates at 179 and 267Hz.

VI. CONCLUSIONS

This paper presents some methods to design notch filters for a prescribed band-reject frequency and 3 dB rejection bandwidth, including of the transfer function design and circuit realization. Then some examples of notch filters at specific frequencies are designed for removing the sinusoidal interference in the servo control system. For simplifying the software computation and the variety natural frequency of mechanical gimbal system, the adaptive notch filter for the arbitrary line-of-sight (LOS) angle should be developed in the control loop. Furthermore, the tracking stability and performance of the servo control system would be corresponding promoted. Finally, the control flow diagram and implementation method of the mechanical gimbal system are given and an experimental example has been illustrated in this paper.

APPENDIX A

Let $V_{X_1} = V_{X_2} = x$, (17) can be reduced to

$$\frac{V_O - x}{R_2} + sC_2\left(V_O - x\right) + sC_1\left(V_i - x\right) = \frac{x}{R_3} \quad \text{(A.1)}$$

By (18),

$$x = \left[\left(1 + R_1 sC_2\right)V_O - V_i\right] \Big/ \left(R_1 sC_2\right) \quad \text{(A.2)}$$

(A.1) multiplies by $R_2 R_3$,

$$V_O R_3 - xR_3 + sR_2 R_3 C_2\left(V_O - x\right) + sR_2 R_3 C_1\left(V_i - x\right) = R_2 x \quad \text{(A.3)}$$

By substituting (A.2) into (A.3),

$$V_O R_3 - \frac{\left(1 + R_1 sC_2\right)V_O - V_i}{R_1 sC_2} R_3 + sR_2 R_3 C_2 V_O - sR_2 R_3 C_2 \frac{\left(1 + R_1 sC_2\right)V_O - V_i}{R_1 sC_2} + sR_2 R_3 C_1 V_i - sR_2 R_3 C_1 \frac{\left(1 + R_1 sC_2\right)V_O - V_i}{R_1 sC_2} = R_2 \frac{\left(1 + R_1 sC_2\right)V_O - V_i}{R_1 sC_2} \quad \text{(A.4)}$$

Separating (A.4),

$$-\frac{V_O R_3}{R_1 sC_2} + \frac{V_i R_3}{R_1 sC_2} - \frac{R_2 R_3 V_O}{R_1} + \frac{R_2 R_3 V_i}{R_1} + sR_2 R_3 C_1 V_i - \frac{V_O R_2 R_3 C_1}{R_1 C_2} - sR_2 R_3 C_1 V_O + R_2 R_3 C_1 \frac{V_i R_2 R_3 C_1}{R_1 C_2} = \frac{V_O R_2}{R_1 sC_2} + V_O R_2 - \frac{V_i R_2}{R_1 sC_2} \quad \text{(A.5)}$$

After (A.5)$\times -sR_1 C_2 \Big/ \left[V_i\left(R_2 + R_3\right)\right]$, (19) can be obtained.

APPENDIX B

By substituting (28) into (26), (26) is separating as

$$V_i - V_{X_3} = V_{X_3} sC_3 R_4 - V_O sC_3 R_4 + V_{X_3} sC_4 R_4 - \frac{sC_4 R_4 R_7 V_i}{R_6 + R_7} \quad \text{(B.1)}$$

Then, according to (27), V_{X_3} is rewritten in

$$V_{X_3} = \frac{R_7 V_i}{R_6 + R_7} + \frac{R_7 V_i}{sC_4 R_5\left(R_6 + R_7\right)} - \frac{V_O}{sC_4 R_5} \quad \text{(B.2)}$$

Thus, by substituting (B.2) into (B.1),

$$\frac{V_O}{V_i}\left\{\frac{1}{C_4 R_5} + \left(\frac{C_3 + C_4}{C_4}\right)\frac{R_4 s}{R_5} + s^2 C_3 R_4\right\} = \frac{R_7}{R_6 + R_7}\left\{\frac{-R_6 s}{R_7} + \frac{1}{C_4 R_5} + s^2 C_3 R_4 + \frac{R_4 C_3 s}{C_4 R_5} + \frac{R_4 s}{R_5}\right\} \quad \text{(B.3)}$$

Finally, (B.3)$\times C_4 R_5$,

$$V_O / V_i = \left[R_7 \Big/ \left(R_6 + R_7\right)\right] \times \frac{C_3 C_4 R_4 R_5 s^2 + \left(R_4 C_3 + C_4 R_4 - \frac{C_4 R_5 R_6}{R_7}\right)s + 1}{C_3 C_4 R_4 R_5 s^2 + \left(C_3 + C_4\right)R_4 s + 1} \quad \text{(B.4)}$$

REFERENCES

[1] Netravali, A. N. “Optimum Digital Filters for Interpolative A/D Convertors,” The Bell System Technical Journal, Vol. 56, No. 9, pp. 1629-1641, 1977.

[2] Daniels, J., Dahaene, W., Steyaert, M. S. J., and Wiesbauer, A., “A/D Conversion Using Asychronous Delta-Sigma Modulation and Time-to-Digital Conversion,” IEEE

Transactions on Circuits and Systems – Part I, Vol. 57, No. 9, pp.2404-2412, 2010.

[3] Caroline, L. P., Petrescu, T., Poulton, D., Duhamel, P., and Oksman, J., "Wideband, Bandpass, and Versatile Hybrid Filter Bank A/D Conversion for Software Radio," IEEE Transactions on Circuits and Systems – Part I, Vol. 56, No. 8, pp.1772-1782, 2009.

[4] Srivastava, V. K. and Ray, G. C., "Design of 2D-Multiple Notch Filter and Its Application in Reducing Blocking Artifact From DCT Coded Image," Proc. IEEE 22nd Annual EMBS International Conference, Chicago, USA, pp. 2829-2833, 2000.

[5] Pei, S. C., Lu, W. S., and Tseng, C. C., "Analytical Two-Dimentionl IIR Notch Filter Design Using Outer Product Expansion," IEEE Transactions on Circuits and Systems – Part II, Vol. 44, No. 9, pp. 765-768, 1997.

[6] Skolnik, M. I., Introduction to Radar Systems, 3rd edition, Boston, Mcgraw-Hill, 2001.

[7] Stimson, G. W., Introduction to Airbourne Radar, 2nd edition, New Jersey, Scitech Publishing, INC, 1998.

[8] Ziegler, M. A., "Design of a Velocity and Position Control Laboratory Servo System," Monterey, Calif. : Naval Postgraduate School, Technical Report, 1987.

[9] Electro-Craft Corporation, "DC Motors, Speed Controls, Servo Systems : An Engineering Handbook," Hopkins, MN : Electric-Craft Corporation ,1975.

[10] Groutage, F. D., "High Torque-to-Interia Servo System for Stabilizing Sensor System：Candidate Systems Include Missle Guidance, Surveillance, and Tracking," Technical Report, July 1979.

[11] Passera, A. L., and Nason, M. L., "The Effect of Control-Surface-Servo Natural Frequency on the Dynamic Performance Characteristics of an Acceleration Control System Applied to a Supersonic Missile," Technical Report, National Advisory Committee for Aeronautics, Washington, 1953.

[12] Analogue-Computer Simulation of an Autopilot Servo System Having Nonlinear Characteristics, Technical Report, National Advisory Committee for Aeronautics, Washington, NOSC, California, 1952.

[13] Sedra, A. S., and Smith, K. C., Microelectronic Circuits, 4th edition, New York, Oxford, 1998.

[14] Coughlin, R. F. and Driscoll, F. F., Operational Amplifiers and Linear Integrated Circuits, 4th edition, Prentice-Hall, New Jersey, 1991.

[15] Lutovac, M. D., Tosic, D. V., and Evans, B. L., Filter Design for Signal Processing Using Matlab and Methematica, New Jersey, Prentice-Hall, 2001.

[16] Boctor, S. A., "Single Amplfier Functionally Tunable Low-Pass-Notch Filter," IEEE Transactions on Circuits and Systems – Part II, Vol. 22, No. 11, pp.875-881, 1975.

[17] Sedra, A. S., and Brackett, P. O., Filter Theory and Design : Active and passive, Portland, Matrix Publishers, 1978.

[18] Daniels, R. W., Approximation Methods for Electronic Filter Design, New York, Mcgraw-Hill, 1974.

[19] Williams, A. B., and Taylors, F. J., Electronic Filter Design Handbook, New York, Mcgraw-Hill, 1988.